ChemComm

COMMUNICATION

View Article Online
View Journal | View Issue

Cite this: *Chem. Commun.*, 2014, **50**, 2100

Received 19th November 2013,
Accepted 18th December 2013

DOI: 10.1039/c3cc48808j

www.rsc.org/chemcomm

Periodical assembly of repetitive RNA sequences synthesized by rolling circle transcription with short DNA staple strands to RNA–DNA hybrid nanowires†

Hong-Ning Zheng, Yin-Zhou Ma and Shou-Jun Xiao*

The long single-stranded RNAs produced from Rolling Circle Transcription (RCT) were used as scaffolds to be folded with a few short DNA staples into RNA–DNA hybrid nanowires.

DNA nanotechnology has been well-developed over the past years,[1] where DNA tiles and origami as building blocks have been extensively explored to be assembled into many well-defined nanostructures. However, its cousin, RNA nanotechnology is still in the period of development. RNA is structurally related to DNA, but exhibits richer chemical, structural and functional diversities, for example loop–loop interaction. In the past decade, two- and three-dimensional RNA nanostructures have already been designed and constructed by various native RNAs and synthetic small RNAs according to loop–loop interaction and Watson–Crick base-pairing (A–U and C–G).[2] With a level of simplicity similar to DNA folding, recently hybrid RNA–DNA nanostructures, including RNA origami with a long RNA strand by transcription folded by short DNA staple strands, have been designed and constructed according to Watson–Crick base-paring (A–T/U and C–G).[3] The potential of both DNA and RNA nano-structures as the genetic vectors and carriers for *in vivo* delivery in therapeutics has been addressed recently, especially taking advantage of the slowing-down degradation of the packed nano-structures.[4] DNA and RNA therapeutics need cost-efficient raw materials. Recently we extended the DNA nanotechnology to a new and cheap source of DNAs by rolling-circle-amplification, where the products of long repetitive single stranded DNAs as scaffolds were folded with a few short DNA staple strands to nano-shapes.[5] Here we present a similar approach to fold long repetitive RNA strands synthesized from rolling circle transcription (RCT)[6] by a few short DNA strands into nanowires.

In the RCT procedure, a single-stranded circular DNA substrate serves as the template for transcription by a RNA polymerase (Fig. 1A). In our case, T7 RNA polymerase was adopted. The polymerase makes a RNA copy of the circular DNA template, and it continues to copy the template sequence without stopping, similar to DNA's rolling circle amplification (RCA). RCT leads to the synthesis of long single-stranded RNAs with hundreds/thousands of copies of a repeating sequence which is the complement of the circular template sequence.

In this communication, we present 4 types of folding strategies for RNA nanowires. Fig. 1A illustrates the whole experimental

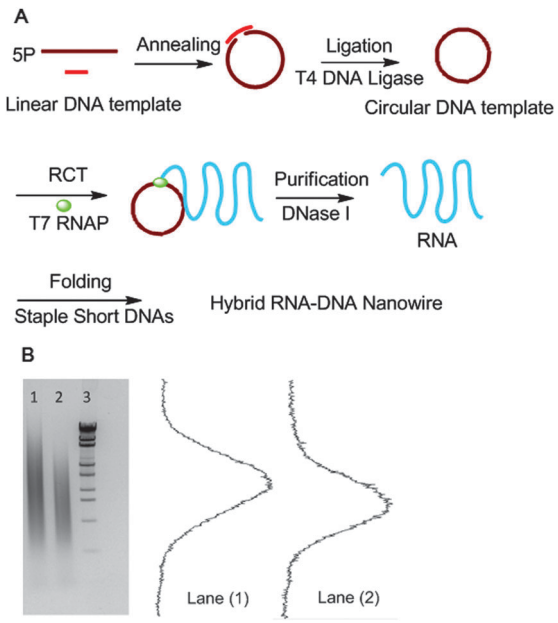

Fig. 1 (A) Schematic representation of the rolling circle transcription (RCT) procedure to produce periodic single RNA sequences and then of folding these RNAs by a few short staple DNAs to hybrid RNA–DNA nanowires. 5P indicates that the linear DNA (brown) was phosphorylated at the 5′-end. (B) (1) Agarose gel (1%) electrophoresis showing the molecular size range of the transcripts: lane 1, RCT products of R1 transcripted from S1 (sequence code see ESI†); lane 2, RCT products of R2 transcripted from S2 (sequence code see ESI†); lane 3, marker ladders: 19 329, 7743, 6223, 4254, 3472, 2690, 1882, 1489, 925, 421 bases. The grey level distributions of lane 1 and lane 2 are depicted in lane (1) and lane (2) respectively.

State Key Laboratory of Coordination Chemistry, School of Chemistry and Chemical Engineering, Nanjing National Laboratory of Microstructures, Nanjing University, Nanjing 210093, Jiangsu, China. E-mail: sjxiao@nju.edu.cn

† Electronic supplementary information (ESI) available: Experimental details and RNA and DNA codes. See DOI: 10.1039/c3cc48808j

procedure. A linear single 96 nucleotide (nt) DNA strand was phosphorylated at the 5′-end. First, the 3′- and 5′-ends of the linear strand were brought together by hybridization with an equal molar short splint and then the nick was chemically closed by T4 DNA ligase. The circular DNA was purified and used as the template for RCT. The RNA transcripts were obtained by *in vitro* transcription with the help of T7 RNA polymerase (T7 RNAP). To testify the feasibility of our thinking, we used two 96 nt DNA sequences: S1 and S2 (sequence codes in ESI†). A T7 promoter sequence is not necessary to be included in the circle sequence, and it does not exist in either of the two sequences we used. The RCT products were analysed by 1% agarose gel as shown in Fig. 1B. The RNA single strands of R1 transcripted from S1 range in length from 421 to 6223 bases (lane 1 in Fig. 1B and its corresponding grey level distribution in lane (1)), and R2 transcripted from S2 range in length from 925 to 6223 bases (lane 2 in Fig. 1B and its corresponding grey level histogram in lane (2)). The RCT products of R1 and R2 are composed of many contiguous periodic complements of S1 or S2 respectively.

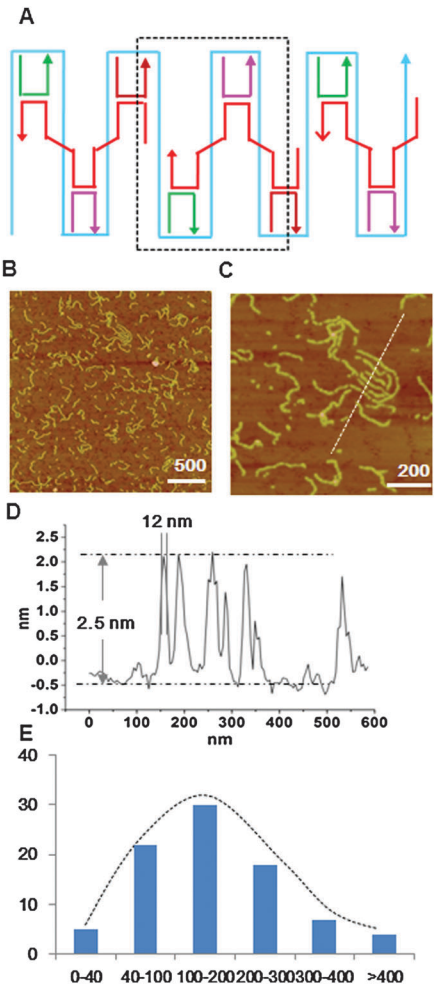

Fig. 2 Folding strategy and AFM images of R1-1 origami. (A) Scheme of folding R1 with 4 staple strands; (B) zoom-out image with a scale bar at 500 nm; (C) zoom-in image with a scale bar at 200 nm; (D) width (12 nm) and height (2.5 nm) of the R1-1 nanowire; (E) statistical length distribution of R1-1 counted from image (B).

All the RNA–DNA hybrid origami nanostructures in this work were designed by following the rules: crossovers spaced every 1.5-turns and odd numbers of half turns each line in the raster. Fig. 2A presents the first design (R1-1): each repeat sequence (96 nt) was folded into 3 equal sections by 4 DNA staple strands (red is 48 nt, pink, green and brown are 16 nt, respectively) into a rectangle (boxed with dotted lines). Then, those rectangles joined together to form a long nanoscale wire. To our knowledge, the double helix of DNA–DNA is prone to form a B-form structure. However an A-form structure is preferred for the hybrid RNA–DNA helix. Since the axial rise per base pair for the A-form RNA–DNA hybrid duplex is 0.28 nm,[7] the width of the nanowire should be the length of 32 base pairs (bp) (~9 nm). Due to the tip effect, the measuring result (12 nm) shown in Fig. 2D was slightly wider than the theoretical value (9 nm). Different from the longer DNA nanowires (several to tens of μm long) formed by rolling circle amplification in our previous report,[5] the RNA–DNA nanowires only exhibit shorter lengths from tens to hundreds of nm. We believe that the shorter nanowires exactly exhibit the feature of single strand RNAs. A simple formula, L1 = 2.5 × (*R*/32) nm, can calculate the nanowire length, where *R* is the number of bases of the RNA scaffold, 2.5 is the diameter of a RNA–DNA hybrid helix in nm. Take Fig. 2A as an example, RNAs of R1 range from 421 to 6223 bases and centered at 1882 bases in Fig. 1B-lane (1), so the RNA nanowires should be in the length range of 33 nm to 486 nm and centered at 147 nm. AFM images of Fig. 2B and C provide direct visualization of the RNA–DNA nanowires. Statistical analysis of the length distribution from Fig. 2B is depicted as a Gaussian distribution histogram in Fig. 2E, which corresponds well to the theoretical estimation by the formula of L1 = 2.5 × (*R*/32).

Additional 3 folding strategies were designed to demonstrate the assembly feasibility of RNA–DNA hybrid origamis. Fig. 3 illustrates a folding strategy (R1-2) similar to R1-1: each 96 × 2 sequences were folded into 6 equal sections as a periodic unit by 6 staple DNA strands (red, blue, violet are 32 nt, and green, pink, brown are 16 nt), where 3 × 32 nt strands replace the one red 48 nt strand shown in Fig. 2A. In this case, the periodic rectangle unit is 2 times that shown in Fig. 2A. Their AFM images in Fig. 3B and C illustrate the same topo-morphologies as shown in Fig. 2B and C because both nanowires were designed to have the same width and length. A similar length distribution is depicted in Fig. 3D.

Furthermore, we changed the circular DNA template sequence from S1 to S2. From the layout of the design (Fig. 4A, named R2-3), each 96 nt RNA chain was folded into 32 bp × 3 helices, and each 96 bp × 2 helices formed a periodic unit (the dotted rectangle box) which was folded by 6 DNA staples (each staple is 32 nt). The theoretical calculation for the length and width of nanowires still agrees with R1-1. AFM images of Fig. 4B and C and the length statistics of Fig. 4B provide a well-predicted histogram in Fig. 4D.

Another folding strategy is illustrated in Fig. 5A (R1-4), each 96 nt RNA was folded into a rectangle of 32 bp × 3 helices with 16 bp × 6 sections (the dotted border in Fig. 5A) by 4 staple strands (red and green are 32 nt, purple and yellow are 16 nt). The RCT products of RNAs continued the same folding

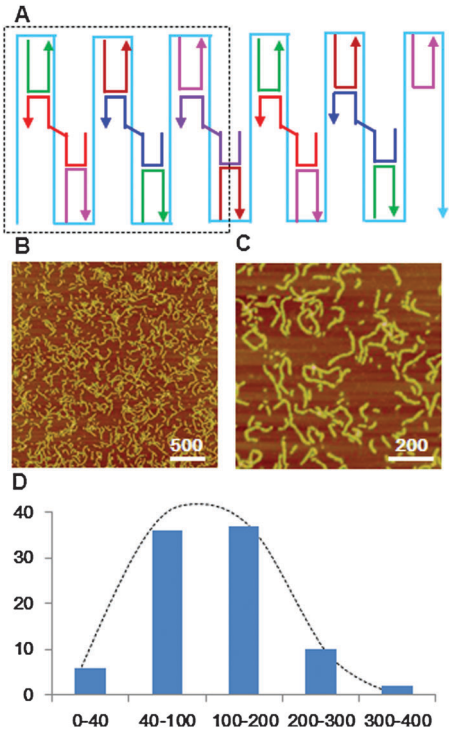

Fig. 3 Folding strategy and AFM images of R1-2 origami. (A) Scheme of folding R1 with 6 staple strands; (B) zoom-out image with a scale bar at 500 nm, (C) zoom-in image with a scale bar at 200 nm; (D) statistical length distribution of R1-2 counted from image (B).

configuration to generate the nanowire with a width of 3 helices, where the difference from Fig. 2A, 3A and 4A is that the double helix axis is parallel to the longitudinal direction of nanowires, while the double helix axis in Fig. 2A, 3A and 4A is perpendicular. In Fig. 5B and C, the width of the nanowires was measured to be around 8 nm, close to the theoretical width of 3 helices at 7.5 nm (2.5 nm × 3). The theoretical length calculation formula in this folding is derived as $L4 = (R/3) \times 0.28$. The statistical distribution from Fig. 5B is plotted in Fig. 5D, which is in agreement with the theoretical estimation.

Given that our AFM images clearly show a large number of individual and non-associated nanowires, the statistical length analyses reveal that all RNA–DNA origami nanowires with lengths in the range of 10 to 500 nm are constructed with individual RNA molecules respectively, different from the RCA DNA–DNA nanowires with tens of micrometre long,[5] which were joint DNA molecules. Even though we have successfully observed RNA–DNA hybrid nanowires with 4 types of folding designs, some questions are still open and need further investigation. For example, high yield RNA transcripts can be generated from the two circular DNA templates of S1 and S2, while low yield RNA transcripts were obtained from other templates; the 2-dimensional RNA–DNA lattice has not yet been observed.

Small RNA molecules such as small interfering RNA (siRNA), ribozyme, antisense RNA and aptamer are attracting more and more attention due to their potential in disease diagnosis and therapeutics ranging from genetic disorders to HIV infection to various cancers.[8] These RNA-based imaging, disease detection,

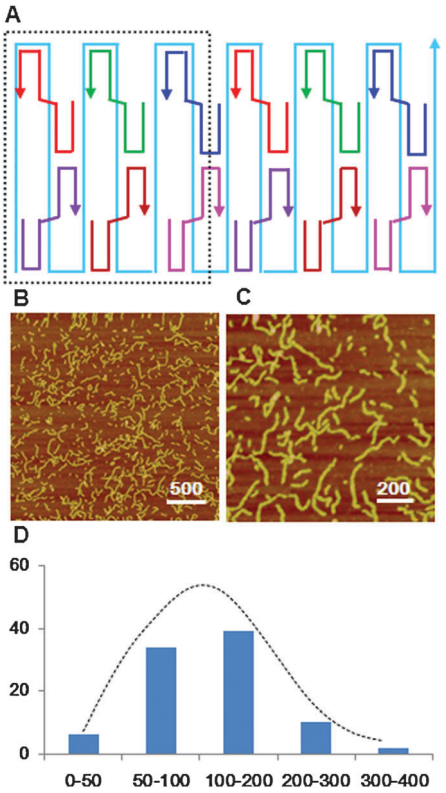

Fig. 4 Folding strategy and AFM images of R2-3 origami. (A) Scheme of folding R2 with 6 staple strands; (B) zoom-out image with a scale bar at 500 nm, (C) zoom-in image with a scale bar at 200 nm; (D) statistical length distribution of R2-3 counted from image (B).

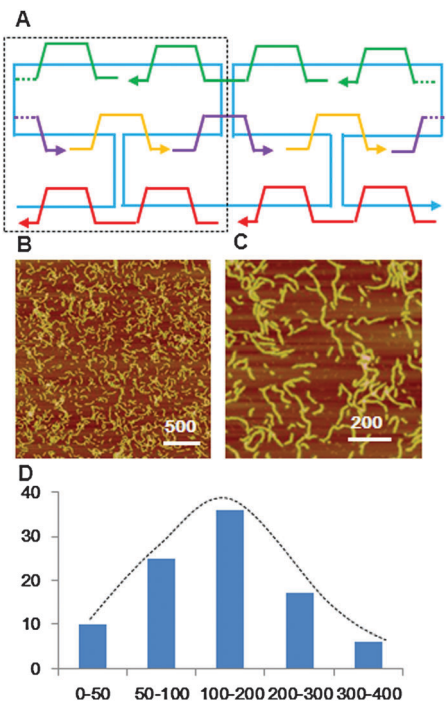

Fig. 5 Folding strategy and AFM images of R1-4 origami. (A) Scheme of folding R1 with 4 staple strands; (B) zoom-out image with a scale bar at 500 nm, (C) zoom-in image with a scale bar at 200 nm; (D) statistical length distribution of R1-4 counted from image (B).

biomarker discovery and drug development demonstrate the unprecedented versatility of RNA. However, RNA is inherently more reactive and labile than DNA *in vivo* due to the plethora of ribonucleases in serum and in cells, and typically needs a delivery carrier for efficient transport to the targeted cells, tissues, or organs. The barrier may be overcome by the emerging RNA nanotechnologies, including closely packed RNA and hybrid RNA–DNA nanoparticles, nano-wires, and nano-devices, which have been demonstrated to degrade slower *in vivo*.[4,8a] The RCT products of repetitive RNA sequences are cost-efficient and easy to prepare. The folded hybrid RNA–DNA nano-wires may provide an easy-access source for RNA therapeutics. On the other hand, the heterogeneity in size of RCT RNA, most likely comprised of multiple configurations each containing different numbers of repeating units or even different degrees of degraded RNA, and hence generating the hybrid RNA–DNA nano-wires in different lengths ranging from 10 to 500 nm, might affect their biomedical functionalities in practice. But, all in all, the long single-stranded RNAs produced by RCT provide a new source for nucleic acid nanotechnology and the folded RNA nanostructures have potential applications in RNA therapeutics, drug/gene delivery, imaging and detection, *etc.*

This work was supported by the financial support of the National Basic Research Program of China, No. 2013CB922101, NSFC, No. 91027019, No. 21021062, and a funding from the State Key Laboratory of Bioelectronics of Southeast University.

Notes and references

1 (*a*) N. C. Seeman, *Annu. Rev. Biochem.*, 2010, **79**, 65–87; (*b*) P. W. K. Rothemund, *Nature*, 2006, **440**, 297–302; (*c*) C. Lin, Y. Liu and H. Yan, *Biochemistry*, 2009, **48**, 1663–1674; (*d*) F. A. Aldaye, A. L. Palmer and H. F. Sleiman, *Science*, 2008, **321**, 1795–1799.

2 (*a*) A. Chworos, I. Severcan, A. Y. Koyfman, P. Weinkam, E. Oroudjev, H. G. Hansma and L. Jaeger, *Science*, 2004, **306**, 2068–2072; (*b*) L. Jaeger and A. Chworos, *Curr. Opin. Struct. Biol.*, 2006, **16**, 531–543; (*c*) P. Guo, *Nat. Nanotechnol.*, 2010, **5**, 833–842; (*d*) G. C. Shukla, F. Haque, Y. Tor, L. M. Wilhelmsson, J. J. Toulmé, H. Isambert, P. Guo, J. J. Rossi, S. A. Tenenbaum and B. A. Shapiro, *ACS Nano*, 2011, **5**, 3405–3418; (*e*) K. A. Afonia, E. Bindewald, A. J. Yaghoubian, N. Voss, E. Jacovetty, B. A. Shapiro and L. Jaeger, *Nat. Nanotechnol.*, 2010, **5**, 676–682; (*f*) I. Severcan, C. Geary, A. Chworos, N. Voss, E. Jacovetti and L. Jaeger, *Nat. Chem.*, 2010, **2**, 772–779; (*g*) C. Geary, A. Chworos and L. Jaeger, *Nucleic Acids Res.*, 2011, **39**, 1066–1080; (*h*) W. Grabow, P. Zakrevsky, K. Afonin, A. Chworos, B. A. Shapiro and L. Jaeger, *Nano Lett.*, 2011, **11**, 878–887; (*i*) D. Shu, W. D. Moll, Z. Deng, C. Mao and P. Guo, *Nano Lett.*, 2004, **4**, 1717–1723.

3 (*a*) S. H. Ko, M. Su, C. Zhang, A. E. Ribbe, W. Jiang and C. Mao, *Nat. Chem.*, 2010, **2**, 1050–1055; (*b*) P. Wang, K. S. Hyeon, C. Tian and C. Mao, *Chem. Commun.*, 2013, **49**, 5462–5464; (*c*) K. Endo, S. Yamamoto, K. Tatsumi, T. Emura, K. Hidaka and H. Sugiyama, *Chem. Commun.*, 2013, **49**, 2879–2881.

4 (*a*) A. V. Pinheiro, D. Han, W. M. Shih and H. Yan, *Nat. Nanotechnol.*, 2011, **6**, 763–772; (*b*) A. Khaled, S. Guo, F. Li and P. Guo, *Nano Lett.*, 2005, **5**, 1797–1808; (*c*) P. Guo, O. Coban, N. M. Snead, J. Trebley, S. Hoeprich, S. Guo and Y. Su, *Adv. Drug Delivery Rev.*, 2010, **62**, 650–666.

5 (*a*) Y. Ma, H. Zheng, C. Wang, Q. Yan, J. Chao, C. Fan and S. J. Xiao, *J. Am. Chem. Soc.*, 2013, **135**, 2959–2962; (*b*) X. Ouyang, J. Li, H. Liu, B. Zhao, J. Yan, Y. Ma, S. J. Xiao, S. Song, Q. Huang, J. Chao and C. Fan, *Small*, 2013, **9**, 3082–3087.

6 (*a*) S. L. Daubendiek, K. Ryan and E. T. Kool, *J. Am. Chem. Soc.*, 1995, **117**, 7818–7819; (*b*) A. M. Diegelman and E. T. Kool, *Nucleic Acids Res.*, 1998, **26**, 3235–3241; (*c*) J. Banér, M. Nilsson, M. Mendel-Hartvig and U. Landegren, *Nucleic Acids Res.*, 1998, **26**, 5073–5078.

7 N. C. Horton and B. C. Finzel, *J. Mol. Biol.*, 1996, **264**, 521–533.

8 (*a*) P. Guo and F. Haque, *RNA Nanotechnology and Therapeutics*, CRC Press, 2013; (*b*) R. Kole, A. R. Krainer and S. Altman, *Nat. Rev. Drug Discovery*, 2012, **11**, 125–140; (*c*) J. C. Burnett and J. J. Rossi, *Chem. Biol.*, 2012, **19**, 60–71.